Synthesis, Crystal Structure, and Physical Properties of $KNa_2[NiO_2]$ and $K_3[NiO_2]$ Containing "Linear" $[NiO_2]^{3-}$ Anions

Angela Möller,*,† Michael A. Hitchman,† Elmars Krausz,‡ and Rudolf Hoppe§

Chemistry Department, University of Tasmania, GPO C252, Hobart, TAS 7001, Australia, Research School of Chemistry, Australian National University Canberra, ACT 2601, Australia, and Institut für Anorganische und Analytische Chemie der Justus-Liebig-Universität, Heinrich-Buff-Ring 58, 35392 Giessen, Germany

Received November 17, 1994[⊗]

The synthesis and the crystal structure refinement for the superstructure of $KNa_2[NiO_2]$ are reported (orthorhombic, *Cmca*, $Z = 8$, $a = 6.261(3)$ Å, $b = 10.474(3)$ Å, $c = 12.472(7)$ Å). It is compared with the subcell, described recently. EPR measurements of powder and single crystal samples of $K_3[NiO_2]$ and $KNa_2[NiO_2]$ are presented, and confirm a $^2\Sigma_g$ ground state for the "linear" $[NiO_2]^{3-}$ complexes in these compounds. Absorption spectra have been measured between 4500 and 20000 cm^{-1}. For the first time both d−d transitions of a "linear" d^9-system are resolved, and the energies of these have been analyzed using the angular overlap model. The near-infrared bands of $K_3[NiO_2]$ exhibit fine structure at low temperature, allowing comparison of the Ni−O symmetric stretching frequencies and bond lengths in the ground and excited states.

1. Introduction

The idea that oxygen would only stabilize high oxidation states in polynary oxides may be regarded as a general guide; examples are $KMnO_4$, K_2FeO_4[1] and Cs_2FeO_4.[2] These and numerous other oxides in more "normal" oxidation states can be synthesized by tempering a mixture of binary oxides in sealed metal containers (e.g. Pt, Au, Fe, Co, Ni, Ag), for example $K_2[NiO_2]$.[3] On the other hand, a reaction with the container wall, normally avoided, presented a new route for a smooth reduction to stabilize "lower" oxidaton states as in the new ternary oxides $RbNa_2[NiO_2]$, $K_3[MO_2]$ (M = Fe, Co, Ni),[4] producing single crystals grown in situ, "out of the wall". These compounds are remarkable not only for the low oxidation state of the metal, but also for the low coordination number, 2.

Another general guide for stabilizing "low" oxidation states of transition metals has been the use of π−acceptor ligands and many examples are found in organometallic chemistry. These niccolates present an interesting system with the π-donor ligand O^{2-}. Moreover, the Ni(I) ion is formally isoelectronic with Cu(II), and the so-called high TC superconductors involve the latter metal interconnected by oxide ions. The magnetic and electrical properties of these novel Ni(I) compounds are therefore of particular interest.

The only other linear 3d transition metal complexes to have been investigated to date are transition metal dihalides, studied either in the gas phase or in matrix isolation studies. However, the lack of comprehensive experimental data, particularly in the near infrared region, has meant that the d-orbital energies for a d^9 system, and even the nature of the ground state, in these molecules have often been the subject of controversy.[5-11] The present study should help to resolve these ambiguities.

Spectroscopic data on $K_2[NiO_2]$, which contains the linear $[NiO_2]^{2-}$ ion, have already been published,[12] providing a useful comparison for some of the properties of the $[NiO_2]^{3-}$ ion. Investigations of the magnetic, optical, and EPR behavior of $K_3[NiO_2]$ and $KNa_2[NiO_2]$ are in progress and initial results are presented here.

2. Experimental Details

Polynary oxides, which contain alkali metals as counterions, are extremely sensitive to air and moisture; therefore, preparations have to be carried out under a dry argon atmosphere. Special equipment is used to handle the compounds.

The following reactants were used for preparing $KNa_2[NiO_2]$: $KO_{0.48}$, controlled oxidation of prepurified potassium metal (Riedel−de Häen) with dried oxygen;[13] Na_2O, reaction of NaOH (p.a. Merck) with sodium metal (98% Riedel−de Häen);[14] CdO (p.a. Merck); "$K_2Na_4CdO_4$", obtained by tempering ground CdO, Na_2O, and $KO_{0.48}$ (molar ratio 1:2:2) at 500 °C (14 d) in sealed Ag-containers as a lemon-yellow crystalline powder, eq 1.

$$K_2O + 2Na_2O + CdO = K_2Na_4CdO_4 \quad (1)$$

Crystalline "$K_2Na_4CdO_4$" was sealed under Ar in Ni-containers and encapsulated in a Supremax glass ampule. This ensemble was tempered for 47 d at 520 °C, in order to achieve a reaction according to eq 2.

* To whom correspondence should be addressed at the Institut für Anorganische Chemie, Universität Hannover, Callinstrasse 9, 30167 Hannover, Germany.
† University of Tasmania.
‡ Australian National University.
§ Justus-Liebig-Universität.
⊗ Abstract published in *Advance ACS Abstracts,* April 1, 1995.

(1) Audette, J. R. et al. *J. Solid State Chem.* **1973**, *8*, 43. Hoppe, M. L.; Schlemper, E. O.; Murmann, R. K. *Acta Crystallogr.* **1982**, *B38*, 2237.
(2) Mader, K.; Hoppe, R. *Z. Anorg. Allg. Chem.* **1991**, *592*, 51.
(3) Nowitzki, B.; Hoppe, R. *Croat. Chem. Acta.* **1984**, *57*, 537.
(4) (a) Burow, W.; Birx, J.; Bernhardt, F.; Hoppe, R. *Z. Anorg. Allg. Chem.* **1993**, *619*, 923; (b) Bernhardt, F.; Hoppe, R. *Z. Anorg. Allg. Chem.* **1993**, *619*, 969.
(5) Kasai, P. H.; Whipple, E. B.; Weltner, W., Jr. *J. Chem. Phys.* **1966**, *44*, 2581.
(6) Houghen, J. T.; Leroi, G. E. James, T. C. *J. Chem. Phys.* **1961**, *34*, 1670. Leroi, G. E.; James, T. C.; Houghen, J. T.; Klemperer, W. *J. Chem. Phys.* **1962**, *36*, 2879.
(7) DeKock, C. W.; Gruen, D. M. *J. Chem. Phys.* **1966**, *44*, 4387.
(8) Lever, A. B. P.; Holleborne, B. R. *Inorg. Chem.* **1972**, *11*, 2183.
(9) (a) Smith, D. W. *Inorg. Chim. Acta* **1971**, *5*, 231. (b) Smith, D. W. *Inorg. Chim. Acta* **1977**, *22*, 107.
(10) Bauschlicher, C. W., Jr.; Roos, B. O. *J. Chem. Phys.* **1989**, *91*, 4785.
(11) Deeth, R. J. *J. Chem. Soc., Dalton Trans.* **1993**, 1061.
(12) Hitchman, M. A.; Stratemeier, H.; Hoppe, R. *Inorg. Chem.* **1988**, *27*, 2506.
(13) Klemm, W.; Wahl, K. *Z. Anorg. Allg. Chem.* **1952**, *270*, 69.
(14) Klemenc, A.; Ofner, G.; Wirth, H. *Z. Anorg. Allg. Chem.* **1951**, *265*, 221.

0020-1669/95/1334-2684$09.00/0

The product, $KNa_2[NiO_2]$, was obtained as dark red columnar shaped single crystals. Cd metal formed via the redox reaction occurred as small pellets which could easily be separated. To obtain $K_3[NiO_2]$ crystalline K_6CdO_4 has been used as a reagent in a similar solid state reaction as described in eq 2 for $KNa_2[NiO_2]$.

$$K_2Na_4CdO_4 + 2Ni = 2KNa_2[NiO_2] + Cd \qquad (2)$$

Single crystals about 0.1 × 0.15 × 0.15 mm^3 in size were selected under an Ar atmosphere in a special apparatus and sealed in quartz capillaries for X-ray diffraction, EPR, and optical investigations.

For optical investigations in the visible and near infrared, the capillaries were mounted on metal plates with a hole of an approximate diameter of 2-3 mm and masked with "blue tac" adhesive putty which was loaded with graphite.

Measurements on the Cary05E spectrophotometer were carried out at room temperature in the region of 5000−20000 cm^{-1} and on a custom-built single beam spectrometer[15] at T = 292, 85 and 6 K, respectively, between 4500−9000 cm^{-1} with a liquid nitrogen cooled InSb and using a Si avalanche detector between 9000−17000 cm^{-1}.

Infrared spectra were measured at room temperature on a Bruker IFS-66 spectrometer with an attached microscope in the region of 600−4800 cm^{-1}. EPR-data were obtained at room temperature at X- and Q-band frequencies on a JEOL JES-FE3X spectrometer.

3. Results and Discussion

3.1. Single Crystal Structure of $KNa_2[NiO_2]$. The crystal structure of $KNa_2[NiO_2]$ was reinvestigated since only the subcell structure could be solved in a previous study (*Cmma*; a = 10.485(3) Å, b = 6.268(1) Å, c = 6.219(1) Å)[4a] which suggested statistical half occupation of the K^+ site.

With the structure refinement on a new single crystal the super-structure (*Cmca*; $a = b_{sub}$, $b = a_{sub}$, $c = 2c_{sub}$) could be solved; see Figure 1a and for further details Tables 1−3. Here a full occupation of the K^+ site is present and two crystallographically independent sites for oxygen occur, so that Ni^+, in contrast to the previous investigation, is coordinated by two different O^{2-} and the $[O1-Ni-O2]^{3-}$ complex anion is slightly bent (175°). Lattice effects due to the different ionic radii of K^+ and Na^+ might be the reason for the distortion of the $[O1-Ni-O2]^{3-}$ unit. Note that two Na−O layers are linked only by Ni^+ ions with Ni−Ni distances of 4.5 Å within one layer and 6.0 Å between two layers separated by alkali and oxygen ions. The coordination polyhedron of the Na^+ ions can be described as a distorted (compressed) tetrahedron, while the K^+ ion is capping a square pyramid of O^{2-} ions belonging to one layer; see Figure 1b.

Table 4 compares MAPLE, the Madelung part of the lattice energy.[19] The difference of both Σ values (1.6%) confirms that the principal features of the constitutions are already mainly presented with this model of the subcell. At the same time it is a warning, because, e.g., the differences of bond length d(Ni−O1) and d(Ni−O2) as well as the angle ∠(O−Ni−O) difference from 180°, are essential for intimate discussion. No calculations are able to replace a thoroughful measurement. Table 5 indicates that the concept of CHARDI,[20] as well as that of VADI,[21] fits quite well, while the concept of Bond Length/Bond Strength[22] does not give such a good agreement.

The differences in the synthesis of $KNa_2[NiO_2]$ previously[4a] and in this work might have an influence on the geometry of

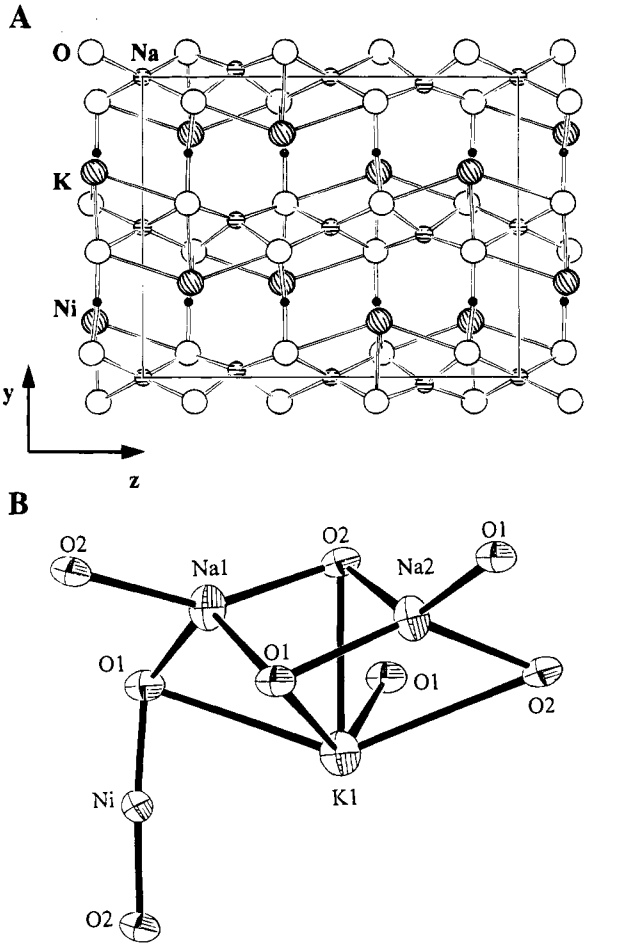

Figure 1. (a) Crystal structure of $KNa_2[NiO_2]$. (b) Part of the structure of $KNa_2[NiO_2]$ illustrating the linking of polyhedra.

Table 1. Crystallographic Data for $KNa_2[NiO_2]$

empicial formula: $KNa_2[NiO_2]$	fw 175.79 g/mol
a = 6.261 (3) Å	space group: *Cmca* (No. 64)
b = 10.474(3) Å	T = 20 °C
c = 12.472(7) Å	λ = 0.710 69 Å (Mo Kα)
V = 817.9(6) Å^3	ϱ_{obsd} = 2.85 g cm^{-3}
Z = 8	ϱ_{calcd}[a] = 3.14 g cm^{-3}
R_{int} = 4.47%	μ = 58.2 cm^{-1}
abs cor,[16] refinement[17]	R = 11.28%[b]
	R_w = 6.66%[c]

[a] Fictive Ni_2O cuprite type (MV = 21.2 cm^3/mol). [b] $R = \Sigma||F_o| - |F_c||/\Sigma|F_o|$. [c] $R_w = \Sigma w^{1/2}||F_o| - |F_c||/\Sigma w^{1/2}|F_o|$.

Table 2. Atomic Parameters and Coefficients of Equivalent Temperature Factors U_{eq}[a] in Å^2 for $KNa_2[NiO_2]$

atom	site	x	y	z	U_{eq}
Ni	8f	0	0.2497(2)	0.3778(4)	0.0210(4)
K	8f	0	0.3144(3)	0.1286(5)	0.0383(10)
Na1	8e	0.25	0.0244(6)	0.25	0.033(3)
Na2	8d	0.267(1)	0.5	0	0.034(3)
O1	8f	0	0.4197(9)	0.363(1)	0.035(4)
O2	8f	0	0.0806(8)	0.380(1)	0.032(3)

[a] $U_{eq} = {}^1/_3(U_{11} + U_{22} + U_{33})$.

The differences in the synthesis of $KNa_2[NiO_2]$ previously[4a] and in this work might have an influence on the geometry of

(15) Krausz, E. *Aust. J. Chem.* **1993**, *46*, 1041.
(16) Walker, N.; Stuart, D. *Acta Crystallogr.* **1983**, *A39*, 158.
(17) Sayre, D. *Acta Crystallogr.* **1952**, *5*, 60. Cromer, D. T.; Mann, J. B. *Acta Crystallogr.* **1968**, *A24*, 321. Sheldrick, G. M. SHELX-76, computer program. Cambridge, England 1976.
(18) Hoppe, R. *Z. Kristallogr.* **1979**, *150*, *23*.
(19) Hoppe, R. *Angew. Chem.* **1966**, *78*, 52; *Angew. Chem., Int. Ed. Engl.* **1966**, *5*, 95; *Angew. Chem. Int. Ed. Engl.* **1970**, *9*, 25; *Adv. Fluorine Chem.* **1970**, *6*, 387; *Izvj. Jugoslav. Centr. Krist.* **1973**, *8*, 21; *Crystal Structure and Chemical Bonding in Inorganic Chemistry*; North Holland Publishing Co., Amsterdam and Oxford; American Elsevier Publishing Co., New York; 1975; p 127.
(20) Hoppe, R.; Voigt, S.; Glaum, H.; Kissel, J.; Müller, H. P.; Bernet, K. *J. Less-Common Met.* **1989**, *156*, 105.
(21) Hoppe, R. To be published shortly.
(22) Brown, I.; Altermatt, D. *Acta Crystallogr.* **1985**, *B41*, 244.

Table 3. Motifs of Coordination Relationships[a] in $KNa_2[NiO_2]$, with Distances in Å and Angles in deg

	O1	O2	CN	ECoN	MEFIR
Ni	1/1	1/1	2	2.0	0.380
	1.790(10)	1.771(9)			
K	1/1 2/2	1/1 1/1	5	4.6	1.606
	3.125(14);	2.790(9);			
	3.321(4)	3.290(14)			
Na1	2/2	2/2	4	4.0	0.951
	2.375(9)	2.329(9)			
Na2	2/2	2/2	4	4.0	0.997
	2.399(10)	2.397(10)			
CN	8	7			
ECoN	6.7	6.4			
MEFIR	1.410	1.391			

O1–Ni–O2	175.0(6)		
O1–K–O1	81.6(2), 81.6(2), 141.0(2)		
O1–K–O2	71.5(3), 70.7(2), 70.7(2), 85.3(2), 85.3(2), 139.8(3)		
O2–K–O2	68.3(3)		
O1–Na1–O1	125.0(4)	O2–Na1–O2	150.7(4)
O1–Na1–O2	98.4(3), 95.0(3), 98.4(3), 95.0(3)		
O1–Na2–O1	105.1(3)	O2–Na2–O2	91.6(3)
O1–Na2–O2	95.9(3), 138.2(3), 95.9(3), 138.2(3)		

[a] For details of the ECoN-concept see ref 18.

Table 4. Madelung Part of Lattice Energy, MAPLE[19] in kcal/mol: A Comparison of the Subcell (*A*)[4a] and the Superstructure (*B*) (this work) of $KNa_2[NiO_2]$

	A	*B*
1 Ni^+	162.3	159.4
1 K^+	72.4[a]	77.2
1 $(Na1)^+$	144.8	148.0
1 $(Na2)^+$	140.8	137.8
1 $(O1)^{2-}$	443.8	428.8
1 $(O2)^{2-}$	443.8	434.4
Σ	1408	1386

[a] Position (8n) for K^+. Statistical distribution delivers distances $d(K-K) \approx 1.40$ Å. To avoid this ordering, it was assumed (if x, y, z occupied, then $-x, y, z$ empty and so on) and correspondingly a ratio of 1:1 of those microdomaines.

$[NiO_2]^{3-}$ observed by X-ray methods as the other details of the two structures like the Na–O layers are almost identical. It is possible that a different cooling rate used in the previous preparation may have caused disorder of the $[NiO_2]^{3-}$ units, so that the apparent linear, centrosymmetric nature reported for these is in fact the statistical average of distorted groups, a twinning problem might have a similar effect. It should be noted that the infrared spectrum of $KNa_2[NiO_2]$ provides confirmation of the distorted nature of the $[NiO_2]^{3-}$ group in this compound; see the following section.

In $KNa_2[NiO_2]$ all $[NiO_2]^{3-}$ units are parallel, whereas in $K_3[NiO_2]$[4b] sheets occur in which the axes of $[NiO_2]^{3-}$ groups are perpendicular, *i.e.* an antiferrodistortive arrangement of the groups in two dimensions. Another difference is that a three-dimensional structure in terms of K^+ and O^{2-} is present in $K_3[NiO_2]$. Note that these structural aspects have to be accounted for the understanding of the physical properties.

3.2. Spectroscopic Studies. We present our initial investigations of the EPR, electronic and vibrational spectra of the $KNa_2[NiO_2]$ and $K_3[NiO_2]$ materials. The results are summarized in Table 6.

3.2.1. EPR Spectra. The EPR spectra of both compounds were measured as powders at X-band frequency, and showed broad intense signals centered at $g \approx 2.3$ (Figure 2). Single crystals were also studied, but because of the orientation of these

Table 5

(a) Charge Distribution (Qc), CHARDI,[20] for $KNa_2[NiO_2]$

	O1	O2	*Q*c(cation)	*V*[a]
Ni	+0.506	+0.494	+1	1.00
	−0.484	−0.516		
K	+0.480	+0.518	+1	0.36
	−0.459	−0.541		
Na1	+0.492	+0.507	+1	0.90
	−0.471	−0.529		
Na2	+0.522	+0.480	+1	0.79
	−0.499	−0.501		
Qc(anion)	−1.91	−2.09	σQc = 0.02%	σV = 7.84%

(b) Valence Distribution (Qv), VADI[21] for $KNa_2[NiO_2]$

	O1	O2	*Q*v(cation)
Ni	0.9997	1.0003	
	−0.5086	−0.4914	
	+0.5081	+0.4922	+1.0003
K	1.7072	1.8917	
	−0.4831	−0.5169	
	+0.4822	+0.5173	+0.9994
Na1	1.9292	2.0664	
	−0.4916	−0.5084	
	+0.4908	+0.5089	+0.9997
Na2	2.0416	1.9568	
	−0.5193	−0.4807	
	+0.5190	+0.4816	+1.0006
*Q*v(anion)	−2.0026	−1.9974	

[a] Bond Length/Bond Strength.[22] From $d(Ni-O) = 1.79/1.77$ Å, we obtained R_{ij} (Ni^{I}) = 1.524 Å in oxides we used here. Note: σQc and σV are the standard deviations with respect to the expected values (oxidation states).

in the quartz capillaries, it was only possible to undertake rotations in the plane perpendicular to the [001] crystal axis for $K_3[NiO_2]$ and [010] for $KNa_2[NiO_2]$, respectively.

For both compounds, the signal was invariant to rotation in the plane specified. Typical spectra for $K_3[NiO_2]$ at Q-band and $KNa_2[NiO_2]$ at X-band are shown in Figure 3. The former compound showed a much broader signal than the latter, and the cause for this difference is unknown. The line width of neither compound altered significantly upon rotation of the crystals. For $KNa_2[NiO_2]$ the linear $[NiO_2]^{3-}$ groups are all parallel to the [010] axis, so that the observed g-value is that perpendicular to the symmetry axis of the complex, $g_\perp = 2.542$. If it is assumed that the powder EPR signal at $g = 2.30$ occurs at approximately the average molecular g-value (*i.e.* $^1/_3(g_\parallel + 2g_\perp)$), this yields the estimate $g_\parallel \approx 1.82$.

For $K_3[NiO_2]$, the symmetry axis of each $[NiO_2]^{3-}$ group lies in the plane perpendicular to [001], but the complexes occur in two sets, with the symmetry axis of one set being perpendicular to that of the other. A single resonance is observed, and as a large anisotropy is expected, the rate of electron exchange between the complexes must be more rapid than the frequency difference between their EPR signals. This can be expected from the significant interactions suggested by the magnetic measurements on the compounds. For $K_3[NiO_2]$, the crystal g-value therefore corresponds to the average of the molecular $g_\parallel$ and $g_\perp$ values. The experimental value, $g \approx 2.2$, can only be obtained approximately because of the sloping base line (Figure 3), but if it is assumed that $g_\perp$ is similar for the two compounds, this implies a value of $g_\parallel \approx 1.9$. This is confirmed by the powder EPR spectrum of $K_3[NiO_2]$. Assuming that the observed signal at $g = 2.31$ occurs at the average molecular g-value yields the values $g_\parallel \approx 1.9$ and $g_\perp \approx 2.5$ for this compound.

The g-values of the $[NiO_2]^{3-}$ group are very similar to those reported for molecular CuF_2 in an argon matrix: $g_\parallel = 1.913$; $g_\perp = 2.601$.[5] This implies a similar electronic ground state in

Table 6. Spectroscopic Data for $KNa_2[NiO_2]$ (I) and $K_3[NiO_2]$ (II)

EPR-data	**(I)**	***observed***	**(II)**	***calculated (k= 0.96)***
powder	$g_{av} = 2.30(2)$		$g_{av} = 2.31(2)$	$g_{av} = 2.33$
crystal	$g_{\perp} = 2.542(4)$		$g_{ex} \approx 2.20$	$g_{\perp} = 2.50$ $g_{\parallel} = 1.98$
VIS-NIR data at		**292 K (I), (II)**		**6K (II)**
crystal		$\Delta E_1 \approx 6000\ cm^{-1}$	$\Delta E_2 \approx 12000\ cm^{-1}$	$\Delta E_1 = 6500\ cm^{-1}$ $\Delta E_2 = 12500\ cm^{-1}$

Estimated Ligand Field σ- and π-bonding parameters

e_{σ}(eff.) = 6250 cm^{-1} $e_{\sigma} = 12000\ cm^{-1}$ $e_{\pi} = 3000\ cm^{-1}$ $e_{ds} = 2875\ cm^{-1}$

Vibrational data	*observed*		*calculated force constants*	
	(I)	**(II)**	**(I)**	**(II)**
	$\nu_s = 668\ cm^{-1}$	$\nu_s = 673\ cm^{-1}$	$f_0 = 4.21$ mdyn/Å	$f_0 = 4.27$ mdyn/Å
	$\nu_{as} = 829\ cm^{-1}$ (broad)	$\nu_{as} = 837\ cm^{-1}$ (broad)	($r_0 = 1.771$ // 1.790 Å)	($r_0 = 1.759$ Å)

Vibrational Energies (ν_s) in the first (1) and second (2) excited states, estimated force constants, bond lengths and displacements in the normal coordinate from relative intensities for $K_3[NiO_2]$

$\nu_{s1} = 600\ cm^{-1}$	$f_1 = 3.40$ mdyn/Å	($r_1 = 1.807$ Å)	$Q_1 = 0.068$ Å	$\delta r_1 = 0.048$ Å
$\nu_{s2} = 535\ cm^{-1}$	$f_2 = 2.70$ mdyn/Å	($r_2 = 1.844$ Å)	$Q_2 = 0.120$ Å	$\delta r_2 = 0.085$ Å

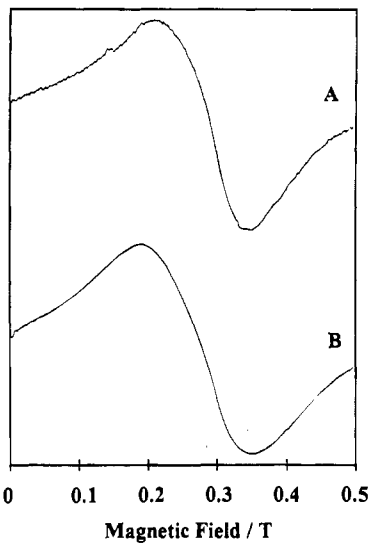

Figure 2. Powder EPR spectrum of $KNa_2[NiO_2]$ (A) and $K_3[NiO_2]$ (B).

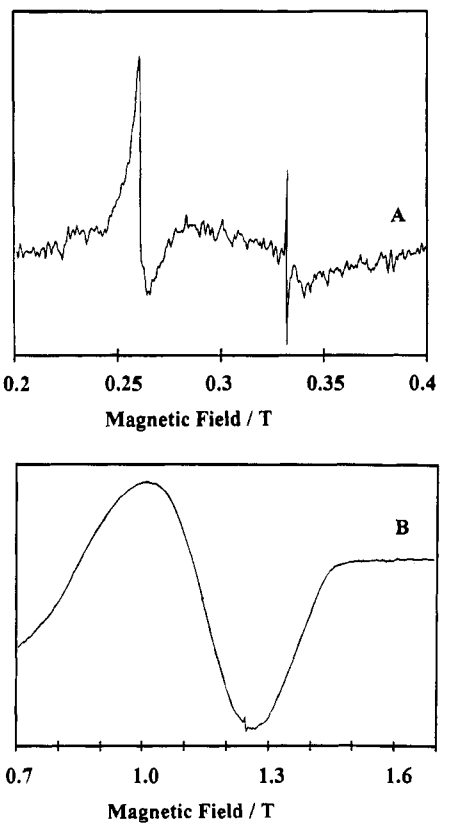

Figure 3. Single-crystal EPR spectrum of $KNa_2[NiO_2]$ (A) at X-band and $K_3[NiO_2]$ (B) at Q-band frequency, with DPPH as a standard.

the two species, confirming the effective oxidation state +1 of the Ni in the former complex. Moreover, the form of the **g**-tensor strongly suggests that, as was inferred for molecular CuF_2, the complex has a $^2\Sigma_g$ ground state, with the unpaired electron localized largely in the d_{z^2} orbital and the significant $g_{\perp}$-shift being caused by spin-orbit coupling to the low-lying $^2\Pi_g$ excited state. It should be noted that the ground state of molecular $CuCl_2$ has been the subject of some controversy. On the basis of molecular orbital calculations it was recently suggested that the ground state is of $^2\Pi_g$ symmetry,[11] and it would be of interest to measure the EPR spectrum of this molecule to test this proposal.

3.2.2. Vibrational Spectra. The infrared spectra of single crystals of the compounds in the range 600−1100 cm^{-1} are shown in Figure 4. A sharp peak is observed at 668 cm^{-1} in the spectrum of $KNa_2[NiO_2]$, the corresponding peak at 673 cm^{-1} being very weak in the spectrum of $K_3[NiO_2]$. This feature is assigned to the totally symmetric Ni−O stretching vibration, which is expected to be infrared inactive for a centrosymmetric $[NiO_2]^{3-}$ group. The relative intensities of this peaks are thus in good agreement with the fact that in $KNa_2[NiO_2]$ the Ni−O bond lengths are inequivalent and the

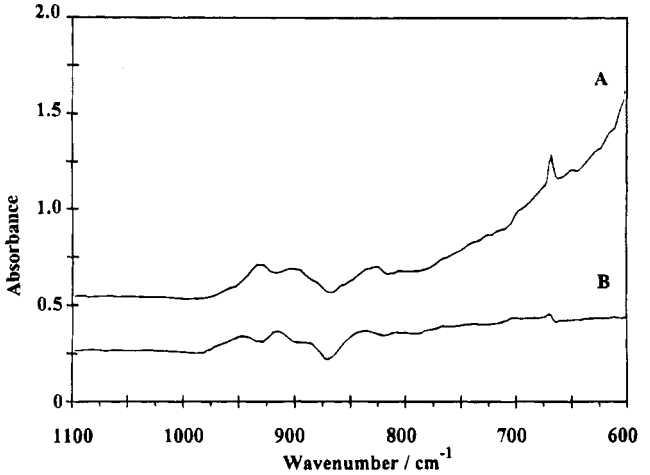

Figure 4. Single-crystal IR spectrum of $KNa_2[NiO_2]$ (A) and $K_3[NiO_2]$ (B).

O−Ni−O angle deviates significantly from 180°. In $K_3[NiO_2]$ the Ni−O bond lengths are crystallographically identical and the $[NiO_2]^{3-}$ group is linear within experimental uncertainty.

The vibrational frequency is a little lower than that reported for the corresponding $[NiO_2]^{2-}$ group in $K_2[NiO_2]$,[12] 733 cm^{-1}. This is in turn consistent with the slightly longer bond lengths in the $[NiO_2]^{3-}$ groups (≈1.76 Å compared with 1.69 Å). The energy of ν_s in the excited electronic states agrees well with the assignment at 668 and 673 cm^{-1} in the ground state (see section 3.2.4).

The calculated force constants for $K_3[NiO_2]$ and $KNa_2[NiO_2]$ are approximately 4.27 and 4.21 mdyn/Å, respectively.

The antisymmetric Ni−O stretching vibration is tentatively assigned to the broad peak observed at ≈830 cm^{-1} in the spectra of both compounds. The peaks lying between 870 and 950 cm^{-1} are probably due to difficulties incurred in the subtraction of the "background" absorption by the quartz capillaries containing the crystals.

The antisymmetric stretch occurs at ≈767 cm^{-1} for CuF_2[5] and 780 cm^{-1} for NiF_2,[23] which agrees well with the assignment of this mode at 830 cm^{-1} for $[NiO_2]^{3-}$ given that oxygen is slightly lighter than fluorine. It is unfortunate that the Raman spectrum of $KNa_2[NiO_2]$ could not be measured as the sample decomposed under laser excitation. Further experiments at low temperature are planned to better define the vibrational spectra of the compounds.

It should be noted that no other bands have been observed between 1100 and 4800 cm^{-1}, specially no O−H vibrations and no bands due to "d−d" transitions as it has been predicted for linear $CuCl_2$ and CuF_2 in this region.[10]

3.2.3. Near-IR/Visible Spectra. The electronic spectra of crystals of $K_3[NiO_2]$ and $KNa_2[NiO_2]$ were measured at room temperature over the range 5000−20000 cm^{-1} with unpolarized light using a Cary 05E spectrophotometer. The small size of the crystals meant that the spectra were of poor quality, though weak bands were observed at ≈6000 and ≈12000 cm^{-1}, with much more intense absorption in the visible region commencing at ≈16000 cm^{-1}. The band intensities were considerably higher for $KNa_2[NiO_2]$ than for $K_3[NiO_2]$, which is consistent with the more highly distorted nature of the $[NiO_2]^{3-}$ group in the former compound.

High absorbances precluded measurement of quantitative spectra for $KNa_2[NiO_2]$. In the case of $K_3[NiO_2]$ a suitable crystal was mounted in a custom-built spectrophotometer, and

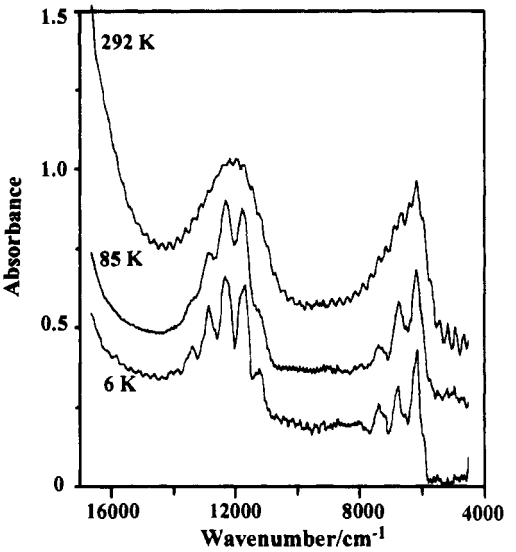

Figure 5. Polarized single-crystal spectra of $K_3[NiO_2]$.

fully resolved spectra were obtained at 292, 85, and 6 K (Figure 5) although fringes arising from the thin double walled capillaries caused some interference. However, bands showing fine structure at low temperature were observed at 6500 and 12500 cm^{-1}. From estimates of the crystal thickness, the extinction coefficient in both bands is ≈5 liter mol^{-1} cm^{-1}. This is quite similar to the intensities reported for the "d−d" transitions of the linear $[NiO_2]^{2-}$ group in $K_2[NiO_2]$.[12] It seems likely that the two bands observed for $K_3[NiO_2]$ are due to "d−d" transitions. The intensity decreases by only a small amount on cooling to 6 K. The bulk of the intensity must be derived either from the asymmetry caused by the slight deviation of the complex from linearity, or from vibronic coupling involving rather high energy vibrations.

The morphology of the crystal was such that the (001) face of the tetragonal unit cell was normal to the light beam. Polarized spectroscopy in this plane is of little assistance in assigning the bands. The axes of the $[NiO_2]^{3-}$ groups lie in this projection of the unit cell, but with those of half the complexes rotated by 90° with respect to those of the other half. The electronic spectra therefore correspond to a superposition of the (**xy**) and (**z**) molecular spectra in both polarizations.

The *g*-values (section 3.2.1) strongly suggest that the complex has a $^2\Sigma_g$ ground state, and the d_{xy}, $d_{x^2-y^2}$ orbitals are effectively non-bonding for a linear complex. The d-orbital energy sequence must be as shown in Figure 7. The highest energy transition at ≈12500 cm^{-1} must therefore occur to the $^2\Delta_g$ state, with the band at ≈6500 cm^{-1} being to the $^2\Pi_g$ state. These transition energies and assignments correspond well with the d-orbital energies deduced for linear $[NiO_2]^{2-}$ [12] and with one assignment of the optical spectrum of molecular $CuCl_2$[7] (see section 3.2.5) and support the predictions for the electronic transitions on the basis of different theoretical models for CuF_2[5,9] and $CuCl_2$.[8] The model used by Roos and Bauschlicher[10] probably leads to a significant underestimate of the first transition energy of CuF_2; moreover, a $^2\Pi_g$ ground state was obtained in the calculation.

The intervals of the structure developing at low temperature, ≈600 and ≈535 cm^{-1} for the lower and higher energy bands, respectively, imply that the band shape is dominated by progressions in the totally symmetric stretching mode. This has a frequency of 673 cm^{-1} in the ground state. This aspect is discussed more fully in section 3.2.4.

The source of the rather intense absorption commencing at about 16000 cm^{-1} in the visible region is of some interest. This

(23) Milligan, D. E.; Jacox, M. E.; McKinley, J. D. *J. Chem. Phys.* **1965**, *42*, 902.

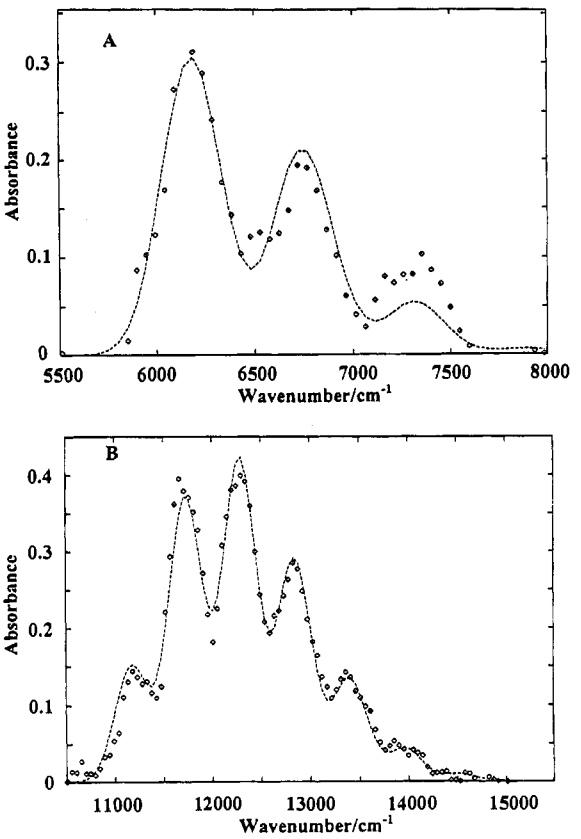

Figure 6. Bandshape analysis for $K_3[NiO_2]$ at 6 K (dashed line, calculated spectrum; square dots, observed data points).

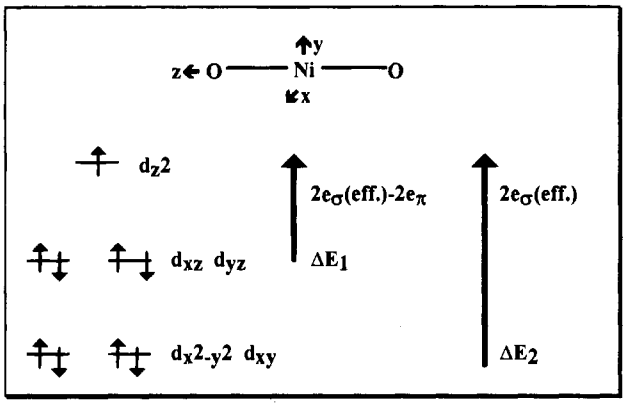

Figure 7. d-Orbital energies for a linear d^9 system.

occurs at considerably *lower* energy for $K_3[NiO_2]$ than for $K_2[NiO_2]$, this trend being the *opposite* of that expected for a ligand → metal charge transfer transition. It therefore seems likely that in the Ni(I) complex, the absorption in the visible region is due to a transition which has considerable metal 3d → 4s character. Because of the low oxidation state of the metal, the 4s orbital is expected to lie at rather low energy and transitions of this type have been characterized in the region 17000–20000 cm^{-1} for several Cu(I) compounds.[24,25]

3.2.4. Fine Structure in the Optical Spectrum of $K_3[NiO_2]$. On cooling from 292 to 85 K, fine structure develops on both "d–d" bands in the crystal spectrum of $K_3[NiO_2]$. This becomes even better resolved on cooling to 6 K (Figure 5). Both bands appear to be dominated by a single progression. The energy increments, ≈600 cm^{-1} for the lower and ≈535 cm^{-1} for the higher energy band, confirm the expectation that this is in the totally symmetric Ni–O stretching vibration. This has an energy of 673 cm^{-1} in the ground state, and this should be reduced in the excited states because of the increase in bond lengths associated with greater antibonding character.

The two "d–d" bands have rather different shapes. That at lower energy is quite asymmetric, as expected for a relatively small change in bond distance, while the higher energy band approximates more closely the symmetrical Gaussian shape which is generally observed when an excited state is substantially displaced from the ground state. The displacements in the normal coordinate Q may be estimated quantitatively from the relative intensities of the members of each progression, and this was carried out by a procedure described previously.[26]

The optimum fits of the relative intensities of each band to one progression based on a single origin are shown in Figure 6. The higher energy band is fitted reasonably well by Q_2 = 0.12 Å. The fit for that at lower energy, obtained with Q_1 = 0.068 Å, is less good.

A factor not included in this treatment is the effect of spin–orbit coupling on the excited states. The CAMMAG[27] calculation (k = 0.96) suggests that this should cause splittings of ≈600 cm^{-1} and ≈1200 cm^{-1} for the $^2\Pi_g(xz,yz)$ and $^2\Delta_g$ (xy,x^2-y^2) states, respectively. The first band does show a second, weaker progression ≈200 cm^{-1} lower in energy than the dominant progression (Figure 5) which could possibly be due to the second spin–orbit member of the $^2\Pi_g(xz,yz)$ state. It is not immediately obvious why the two components should have different intensities.

For the $^2\Delta_g(xy,x^2-y^2)$ state, the spectrum shows no clear evidence of a second progression. It is conceivable that here the spin-orbit splitting is close to the vibrational energy, ≈535 cm^{-1}, and the observed bandshape could be fitted satisfactorily on this basis with a displacement Q = 0.105 Å, slightly less than that giving the optimum fit assuming a single progression. In any event, it seems that for both excited states the effective spin–orbit coupling constant is reduced to less than half the free ion value.

While this might conceivably be due to the quenching of orbital momentum because of a distortion in the excited state (a so-called "Ham effect"),[28] this seems unlikely, particularly for the $^2\Delta_g(xy,x^2-y^2)$ state, since this is formally nonbonding. The possibility that the band at 12500 cm^{-1} is in fact due to a transition which is largely d_{z^2} → 4s in character cannot be ruled out entirely, as this would not exhibit a spin–orbit splitting. However, such an assignment seems unlikely in view of the low energy and weak intensity of the band.

It must also be recognized that the present treatment assumes that each progression is effectively built upon a single origin. If significant intensity is derived from vibronic coupling, each band will be built upon a different vibronic origin in each molecular polarization. As the spectrum of the present crystal is the sum of the **xy** and **z** spectra, each band is expected to consist of two progressions, separated by the difference in energy between the ungerade vibrations. Possibly the second weak progression in the band at 6500 cm^{-1} is caused by this effect. However, as neither the activity of the two modes in inducing intensity, nor the energy of the bending vibration, are known, this aspect cannot be properly explored until the molecular polarized spectra can be resolved, and we are

(24) Jansen, M. *Angew. Chem.* **1987**, *99*, 1136.
(25) Vitale, M.; Palke, W. E.; Ford, P. C. *J. Phys. Chem.* **1992**, *96*, 8329.
(26) Hitchmann, M. A. *Transition Metal Chemistry*; Marcel Dekker, Inc.: New York, Basel, 1985; Vol. 9, 58 ff.
(27) Cruse, D. A.; Davis, J. E.; Gerloch, M.; Harding, J. H.; Mackey, D. J.; McMeecking, R. F. CAMMAG, a FORTRAN computing package. University Chemical Laboratory, Cambridge, England 1979.
(28) Ham, F. S. In *Electron Paramagnetic Resonance*; Geschwind, S., Ed.; Plenum: New York, 1972; p 1.

currently attempting to grow crystals with a morphology which will allow this.

With the above limitations in mind, the bond length changes implied by the above bandshape analyses may be compared with those observed for other systems. For a linear complex, the change in bond length, δr, is related to the displacement in the totally symmetric normal coordinate Q by:

$$\delta r = Q/\sqrt{2} \tag{3}$$

The analysis thus suggest $\delta r_1 \approx 0.048$ Å for the first excited state, and $\delta r_2 \approx 0.085$ Å for the second band, assuming that this is due to a single progression. The significantly larger displacement in the $^2\Delta_g(xy,x^2 - y^2)$ state is consistent with the greater antibonding character of this compared with the $^2\Pi_g$-(xz,yz) state. The displacements are similar to those derived from analysis of the spectra of a number of complexes, where δr ranges from 0.03 to 0.11 Å.[29]

It has been proposed[29] that the change in bond length accompanying the rearrangement of the d-electrons in a transition metal complex is given approximately by the following expression:

$$\delta r \approx nm\Delta/(rfN) \tag{4}$$

This has been found to give good agreement with the experiment for several planar, octahedral and tetrahedral complexes. Here m is the number of electrons involved in the change, 1 in the present case, N is the number of ligands, 2 for a linear complex, Δ the energy difference between the states, r_o the initial bond distance, 1.759 Å for $K_3[NiO_2]$, and f the force constant of the vibration involved in the change of geometry.

It is assumed that Δ varies inversely as the nth power of the bond length, and for octahedral complexes both theory and experiment[30] suggest that $n \approx 5$. Substituting this value and f = 4.27 mdyn/Å (2.15 × 10^5 cm^{-1} Å^{-2}) into eq 4 yields $\delta r \approx$ 0.045 for the $^2\Pi_g(xz,yz)$ state (Δ = 6500 cm^{-1}), and 0.086 Å for the $^2\Delta_g(xy,x^2 - y^2)$ state (Δ = 12500 cm^{-1}), in excellent agreement with the values derived from the band shape analysis, ≈0.048 and ≈0.085 Å, respectively. It appears that the above expression gives reasonable estimates of the bond length changes accompanying electron excitations of these linear complexes, so that it is applicable to a wide range of geometries and coordination numbers. As expected, the vibrational energies, ≈673, 600, 535 cm^{-1} decrease significantly as the Ni−O bond lengthens from 1.759 to ≈1.807 to ≈1.844 Å.

3.2.5. Bonding Parameters. The metal−ligand interaction in the $[NiO_2]^{3-}$ group is here conveniently discussed using the angular overlap model (AOM) of the bonding in transition metal complexes.[31] Assuming δ-interactions are negligible, the d-orbital energies may be expressed in terms of σ- and π-antibonding parameters e_σ and e_π. For a linear complex the d_{xy}, $d_{x^2-y^2}$ orbitals are nonbonding, and the other d-orbitals have the energies (eq 5):

$$d_{z^2} = 2e_\sigma(\text{eff}); \; d_{xz}, d_{yz} = 2e_\pi \tag{5}$$

Here, e_σ(eff) represents both the σ-interacton with the ligand orbitals, given by e_σ, and the effect of configuration interaction between the d_{z^2} orbital and the metal 4s orbital, conventionally represented by the parameter e_{ds}. For a linear complex these are related by eq 6.

$$e_\sigma(\text{eff}) = e_\sigma - 2e_{ds} \tag{6}$$

The above assignment of the excited states means that the energy of the band at ≈12500 cm^{-1} yields the value e_σ(eff) ≈6250 cm^{-1} directly, as as the energy of the lower energy band, ≈6500 cm^{-1}, equals ($2e_\sigma$(eff) − $2e_\pi$) this leads to the estimate $e_\pi \approx 3000$ cm^{-1} (Figure 7). These values are quite similar to those derived for the corresponding Ni(II) complex, $[NiO_2]^{2-}$,[12] where e_σ(eff) ≈ 6500 cm^{-1} and $e_\pi \approx 3500$ cm^{-1}. As expected, smaller bonding parameters occur when the metal is in the lower oxidation state, though the difference is minimal.

The comparatively low value of the ratio e_σ(eff):e_π in these complexes, ≈1:2, is most likely due to the depression of the d_{z^2} orbital by d−s mixing. This is proportional to the difference between the axial and in-plane metal−ligand interaction, which is very large for a linear complex.

More direct evidence for this effect comes from the metal hyperfine coupling constants derived from the EPR spectra of tetragonally compressed octahedral Cu(II) complexes.[32] Here, it has been concluded that the unpaired electron typically spends ≈3.2% of its time in the 4s orbital, though in the linear CuF_2 molecule, which represents the limiting case for a tetragonal compression, this rises to ≈25%.[5]

For octahedral and planar complexes, the e_σ:e_π ratio is typically ≈1:4.[33] If a similar ratio is assumed for the linear complexes, eqs 5 and 6 imply values of e_{ds} of ≈3750 and ≈2875 cm^{-1}, and a depression of the d_{z^2} orbital of ≈15000 and ≈11500 cm^{-1} for $[NiO_2]^{2-}$ and $[NiO_2]^{3-}$, respectively. For the former complex, it was pointed out that if the metal 4s orbital is ≈80000 cm^{-1} above the d-orbitals, simple perturbation theory implies ≈20% fractional occupancy of this orbital in the half-filled Σ_g-(z^2) orbital, in good agreement with estimate of ≈25% from the EPR spectrum of CuF_2.[5]

If, as seems likely, the d−s separation is much smaller in $[NiO_2]^{3-}$, this implies an even larger s participation in the ground state wavefunction; an energy separation of ≈30000 cm^{-1} suggests approximately 40% s character. However, it must be stressed that these numbers are based upon crude approximations. At the very short bond lengths observed for the linear complexes, the e_σ:e_π ratio may be significantly lower than that deduced for octahedral and planar complexes, which would mean that the effects of d−s mixing are overestimated in the above analysis.

However, it seems safe to conclude that configuration interaction between the 4s and d_{z^2} orbitals is significant in these linear complexes, and that this leads to a considerably larger participation of the 4s orbital in the ground state wave function for the Ni(I) complex compared with Ni(II). The diffuse nature of the 4s orbital, combined with the fact that this leads to a substantial contribution to the ground state wave function and a presumably high electron density on the ligands, may contribute to the mechanism producing the strong magnetic coupling which is observed for the Ni(I) complexes[34] despite the lack of any apparent superexchange pathway.

The effect of the deviation from linearity upon the energy levels of the complex in $KNa_2[NiO_2]$ was investigated using the computer program CAMMAG developed by Gerloch and co-workers.[27] This calculates the energy levels of a complex

(29) Hitchmann, M. A. *Inorg. Chem.* **1982**, *21*, 821.
(30) Smith, D. W. *J. Chem. Phys.* **1969**, *50*, 2784. Bermejo, M.; Pueyo, L.; *J. Chem. Phys.* **1983**, *78*, 854. Drickamer, H. G. *J. Chem. Phys.* **1967**, *47*, 1880.
(31) Schäffer, C. E.; Jørgensen, C. K. *Mol. Phys.* **1965**, *9*, 401. Reference 1 Chapters 1, 3, and 9.
(32) Hitchman, M. A.; McDonald, R. G.; Reinen, D. *Inorg. Chem.* **1986**, *25*, 519.
(33) Bencini, A.; Benelli, C.; Gatteschi, D. *Coord. Chem. Rev.* **1984**, *60*, 131. Smith, D. W. *Struct. Bond.* **1972**, *12*, 50.
(34) Murray, K. Private communication.

within the framework of the AOM using the ligand positions indicated by the crystal structure. The only significant result of the bending was a splitting of the $^2\Pi_g(xz,yz)$ state, though the magnitude of this, $\approx$70 cm^{-1}, was too small to be detectable. The inclusion of separate bonding parameters to account for the slight difference in the Ni−O bond distances has no significant effect on the calculation, as for an almost linear complex, the metal experiences the average effect of the ligands. Inclusion of the spin−orbit coupling constant appropriate to Ni^+, 588 cm^{-1}, in the calculation produced g-values ($g_{\|} = 1.98$; $g_{\perp} = 2.50$) in reasonable agreement with those observed experimentally ($g_{\|} \approx 1.9$, $g_{\perp} \approx 2.5$). However, the orbital reduction parameter required for this, $k = 0.96$, is unreasonably large, at least as far as a simple ligand-field picture of the bonding is concerned.

Not only should k be reduced from unity by delocalization of the unpaired electron onto the ligand orbitals, but also because the substantial metal 4s contribution to the ground state wavefunction should make no contribution to the orbital angular momentum. However, it has been shown that the unpaired spin density on the ligands can have a significant influence on the **g**-tensors of complexes, and possibly this affects the k value in the present case. We are currently carrying out molecular orbital calculations to investigate the origin of the g−shift in more detail. The CAMMAG calculations suggest that spin−orbit coupling is also expected to produce a significant splitting of both excited states, and this is considered in section 3.2.4.

The assignment of the electronic spectrum and metal−ligand bonding parameters of the linear molecular $CuCl_2$ have been the subject of considerable controversy. The spectrum exhibits bands at $\approx$9000 cm^{-1} and $\approx$18000 cm^{-1}. Initially, these were assigned to transitions to the $^2\Pi_g$ and $^2\Delta_g$ states, respectively, and this led to the derivation of the AOM bonding parameters e_σ(eff) $\approx$ 8500 cm^{-1} and e_π 3500 cm^{-1},[9a] the σ-parameter being significantly larger than that of the oxide ligands in the present study. Subsequently, the higher energy band was assigned to a charge transfer transition, with the transition to the $^2\Delta_g$ state being at $\approx$9000 cm^{-1}, and it was inferred that the $^2\Pi_g$ state lies at 3300−5000 cm^{-1},[7,8,9b] too low in energy to be observed. This leads to bonding parameter e_σ(eff) $\approx$ 4500 cm^{-1}, $e_\pi \approx$ 2400−3300 cm^{-1}, which are similar to, though somewhat lower than, the values deduced for the linear Ni(I) and Ni(II) oxide ions. This might be due to a longer metal−chlorine bond (d(M−Cl) $\approx$ 2.10 Å).

Recently, two detailed molecular orbital calculations on $CuCl_2$ have been reported. While these differ significantly in the predicted excited state energies, both suggest a $^2\Pi_g$ ground state for the molecule, implying that the chloride ligands exert an extremely strong π−interaction.[10,11] This appears to contradict both the present results on the linear nickel oxides, and the EPR data on molecular CuF_2,[5] since both oxide and fluoride are expected to be stronger π-donors than chloride. While the question would be resolved best by measuring the EPR spectrum of $CuCl_2$, we are currently undertaking detailed molecular orbital calculations on the linear nickel oxides to allow comparison with the studies of $CuCl_2$.

4. Summary

The EPR spectra of $K_3[NiO_2]$ and $KNa_2[NiO_2]$ are characteristic of compounds with a single unpaired electron and confirm the monovalent state of Ni. The **g**-tensors are very similar to that reported for molecular CuF_2,[5] which is isoelectronic with the $[NiO_2]^{3-}$ ion, and imply that the linear complexes have ground states of $^2\Sigma_g(d_z^2)$ symmetry, though this wave function appears to have a substantial contribution from the metal 4s orbital. Significant 4s−3d_{z^2} mixing is suggested by the energy of the $^2\Delta_g(xy,x^2 - y^2)$ excited state, which is considerably lower than might be expected. In addition, it seems likely that the intense absorption of the compounds in the visible region is due to a transition to an orbital with significant 4s character.

Preliminary measurements of the magnetic susceptibility of the compounds give evidence of strong magnetic interactions, despite the absence of any obvious direct or superexchange pathways. Possibly, the participation of the 4s orbital in the ground state is important in the exchange mechanism, as this orbital is expected to be very diffuse because of the low oxidation state of the metal. Further studies of this aspect are in progress.

The $^2\Pi_g(xz,yz)$ excited state energy implies a strong metal−ligand π-interaction, as might be expected from the very short Ni−O bond lengths. The form of the fine structure observed on both "d−d" bands of $K_3[NiO_2]$ at low temperature suggests an increase in Ni−O bond length in each excited state in good agreement with theory. The decrease in energy of the symmetric stretching vibration compared with that in the gound state is consistent with these bond length changes. An unexplained feature of the optical spectrum is the small splitting due to spin−orbit coupling in both excited states. It is hoped to clarify this aspect by growing crystals with a morphology which will allow the separation of (molecularly) polarized spectra of the chromophoric units within the crystal.

Acknowledgment. The receipt of a Research Fellowship from the Deutsche Forschungsgemeinschaft (DFG), Bonn, Germany is gratefully acknowledged by A.M. Dr. Horst Stratemeier is thanked for carrying out the band shape analysis.

Supplementary Material Available: Tables of crystal data, atomic coordinates, bond lengths and angles, coefficients of the anisotropic temperature factors and a labeled figure of **1a** are included for $KNa_2[NiO_2]$ (7 pages). Ordering information is given on any masthead page.

IC941311B